designs

MDPI

Article

CFD Simulations of Single- and Twin-Screw Machines with OpenFOAM

Nicola Casari [1,*], Ettore Fadiga [1], Michele Pinelli [1], Alessio Suman [1] and Davide Ziviani [2]

[1] Department of Engineering (DE), University of Ferrara, Via Saragat 1, 44122 Ferrara (FE), Italy; ettore.fadiga@unife.it (E.F.); michele.pinelli@unife.it (M.P.); alessio.suman@unife.it (A.S.)

[2] Ray W. Herrick Laboratories, Purdue University, 177 S. Russell St., West Lafayette, IN 47907-2099, USA; dziviani@purdue.edu

* Correspondence: nicola.casari@unife.it; Tel.: +39-0532-974964

Received: 10 October 2019; Accepted: 25 January 2020; Published: 30 January 2020

Abstract: Over the last decade, Computational Fluid Dynamics (CFD) has been increasingly applied for the design and analysis of positive displacement machines employed in vapor compression and power generation applications. Particularly, single-screw and twin-screw machines have received attention from the researchers, leading to the development and application of increasingly efficient techniques for their numerical simulation. Modeling the operation of such machines including the dynamics of the compression (or expansion) process and the deforming working chambers is particularly challenging. The relative motion of the rotors and the variation of the gaps during machine operation are a few of the major numerical challenges towards the implementation of reliable CFD models. Moreover, evaluating the thermophysical properties of real gases represents an additional challenge to be addressed. Special care must be given to defining equation of states or generating tables and computing the thermodynamic properties. Among several CFD suite available, the open-source OpenFOAM tool OpenFOAM, is regarded as a reliable and accurate software for carrying out CFD analyses. In this paper, the dynamic meshing techniques available within the software as well as new libraries implemented for expanding the functionalities of the software are presented. The simulation of both a single-screw and a twin-screw machine is described and results are discussed. Specifically, for the single-screw expander case, the geometry will be released as open-access for the entire community. Besides, the real gas modeling possibilities implemented in the software will be described and the CoolProp thermophysical library integration will be presented.

Keywords: CFD; positive displacement machines; OpenFOAM; dynamic mesh

1. Introduction

Positive Displacement machines (PDMs) play a crucial role in a huge number of applications. Air compression, vapor compression, and Organic Rankine Cycles (ORCs) are just few examples in which PDMs are widely employed. These machines are typically preferred to dynamic machinery for a number of reasons including high pressure ratio preserving compactness, unsteadiness of the working conditions, and low enthalpy jump can cause dramatic efficiency losses [1,2]. Within this framework, the performances of PDMs are receiving growing attention by the researchers.

Among the several types of PDMs, screw-type machines are one of the most used devices. Cost-effectiveness, compactness, and quietness are just a few of the reasons that have helped in making these machines so popular [3–6]. These devices have received an increasing interest, making screw compressors to comprise the majority of all positive displacement compressors in operation, as reported by [7,8]. The massive usage of these machines and regulations aiming to more efficient usage of energy [9] led researchers to look into the design phase and the operation analysis of screw-machines in

order to maximize its efficiency. Analytical [10], experimental [11] and computational [12,13] analyses have been proposed in the literature in order to understand the fluid-dynamics inside the machines.

The Computational Fluid Dynamics (CFD) analysis [3,14–16] is a useful tool for the prediction of flow behavior and performance: the geometry complexity and the compatibility of the instrumentation make the experimental campaign very challenging. Sometimes the numerical approach is the only way to investigate the potential behaviour of PDMs with different fluids, without major changes to the plant to be carried out. The complexity of the problem has brought about the application of several numerical strategies to solve the behaviour of volumetric machinery. Among the others, single-screw compressors and expanders are particularly challenging to be simulated. Specifically, the definition of a structured grid compatible with the rotor displacement is not straightforward. Such a mesh could bear the high deformation and the stretch imposed by the motion without seeing a drop in the cell quality. Indeed few attempts in the literature have been done in simulating such machinery, basically taking advantage of overset grids [14].

In this article, many approaches for the analysis of single and twin-screw machines through CFD are illustrated. All the possible approaches that come with the open-source software OpenFOAM-v1806, OpenFOAM-6 and the extended version foam-extend 4.0 have been tested on the case study. The peculiarities of all the studied techniques are reported and the main features of each approach are highlighted.

Open-source CFD suites are gaining more attention by companies and researchers as they are showing capabilities comparable with commercial tools. This work aims to assess the capability of the widely known open-source opensource CFD software in simulating PDMs. As the same setup (in terms of mesh quality, mesh motion, operating conditions) has proven to work with other proprietary CFD suites, the state of the art with OpenFOAM is presented. The user should consider this paper as an overview of the possible techniques to be used for the CFD analysis of the screw-type machines and the mesh requirements for being able to run such a simulation. Pros and cons of each method are described and the most promising methodology is suggested. Furthermore, a new approach based on an external mesh generator is employed. Also, the thermophyisical properties modeling details are reported as well.

The numerical approaches investigated for the single screw simulation have been divided according to the requirement of mesh deformation. Mesh Adaption—dynamic remeshing and Key Frame Remeshing require the mesh to follow the evolution of the fluid domain and therefore ask for mesh deformation. On the other hand, Immersed boundary and Overset grids are rigidly displaced: the actual evolution of the flow field is obtained by means of activating only the computational cells that lay inside the actual fluid domain. A different approach is proposed for the twin screw simulation. The method, belonging to the mesh morphing category, relies on the a-priori definition of the points location during the evolution. All of these methods will be described in the following.

The approach chosen for the simulation must cope with the thermophysical models for the elaborated fluid. As the vast majority of the applications in which PDMs are used exploits phase change for power generation or cooling, the working points in which they operate is close to the saturation dome. As the critical point is approached, the ideal gas model does not hold. Considering the gas to have the ideal behaviour (neglecting inter-molecular force effects) in the proximity of the critical point can lead to deviations up to the 12% in the performance prediction, as reported by [2].

The appropriate model of real gas should rather be chosen, according to experimental data available or comparison with numerical code that implement the Helmholtz equation [17]. In this work, the real gas modeling possibilities available with the software are described. These include typical cubic equations of state (Peng-Robinson [18], Redlich-Kwong [19], Aungier-Redlich-Kwong [20], Soave-Redlich-Kwong [21]) and a new functionality of the software that implements a CoolProp wrapper for OpenFOAM is presented [22].

2. Mesh Moving Techinques in OpenFOAM and Analysis of Single—Screw Expanders

2.1. Creating the Mesh

The workflow for the CFD analysis of a single screw expander (SSE) starts with the definition of a proper mesh generator able to provide meshes that are suitable for the motion technique that will be employed.

OpenFOAM provides a built-in mesh generator, *snappyHexMesh*, which is designed for meshing complex geometries with a cut-cell approach [23]. The resulting mesh is a hex-dominated mesh, with polyhedral cells close to the walls. cfMesh [24] is another mesh generator that has been fully integrated with OpenFOAM. This application is able to generate hex-dominated meshes, but also tetrahedral and polyhedral meshes. The mesh parameter definition and the generation are faster than the first method, even though the quality is generally slightly lower with respect to the former case.

External generators can be used as well, thanks to the utilities for the mesh conversion. Either proprietary software or open-source applications can be used. For example, *fluent3DmeshToFoam* or *gambitToFoam* can be used for mesh prepared with ICEM-CFD or ANSYS-GAMBIT. Typical open-source mesh generators compatible with the CFD solver are salome-platform [25] from OPEN-CASCADE and Gmsh [26]. All the mesh generation techniques described above are available in all the different branches of OpenFOAM.

2.2. Moving the Mesh—Numerical Strategies Available

The choice of the mesh depends on the motion technique to be adopted. The different mesh motion techniques available with the software suite are divided according to the requirement of cell deformation: rigid mesh motion techniques and mesh deformation approaches. Immersed Boundary Method (IBM) and Overset grid belong to the first category, where no deformation is required. The update of the fluid domain according to the operation of the machine relies on different techniques. On the other hand, Mesh Adaption—Dynamic Remeshing and Key Frame Remeshing rely on the deformation of the grid: the operation of the machine is intrinsically evaluated by updating the cells close to the wall. Indeed, this includes a term for the boundary displacement that is plugged in as boundary condition for the solution of the flow [27]. In the following, a brief overview of each of the methods is provided.

2.2.1. Rigid Mesh Motion—IBM

The IBM technique, firstly proposed by [28], is a CFD approach in which the computational domain does not conform to the solid boundary. This represents indeed an advantage because the time-consuming grid generation procedure can be extremely fast. In this case, the imposition of the boundary conditions implies a modification of the governing equations, adding a source term. Such procedure is typically referred to as forcing [29], and in OpenFOAM the forcing operation is done on the discretized equations. For this reason, the approach implemented in the software is called discrete forcing [30].

At the moment, this approach is only available within the extended version of OpenFOAM (i.e., foam-extend from version 3.2 onward). The mesh can be obtained from snappyHexMesh, using only the castellated step without getting rid of the "solid" domain. The mesh motion is implemented as well, by an update of the boundary conditions accordingly. In order to have a better representation of the flow close to the boundary mesh can be refined around the theoretical position of the boundary for each time step, by means of the *refineImmersedBoundaryMesh* utility.

To the scope of the PDM modeling, the application of IBM is not fully applicable. Indeed, at the current state of the art, the implementation in foam-extend does not provide support for compressible flows. Therefore, a little bit of coding is required for the modeling of SSE. The other cons of this technique are related to the poor resolution of the boundary layer. This problem is intrinsic to the method, not to the implementation in OpenFOAM. The first grid close to the wall is not guaranteed to

be aligned with the boundary itself (as it is typically in body-fitted grid). This is generally related to an extra diffusivity that is not physical and can only be reduced (not eliminated) by increasing the order of accuracy of the simulation.

2.2.2. Rigid Mesh Motion—Overset

The overset mesh strategy is based on the application of the Finite Volume Method (FVM) to overlapping grids. This approach was firstly proposed in [31], and further refined in [32]. One or more overset grids, which discretize the moving bodies, are stacked on a background mesh that models the fixed regions of the computational domain. One of the advantages of this approach is the avoidance of mesh deformation during the transient calculation of moving domains. This technique is based on the simultaneous use of active, passive and interpolating cells. In the active cells, the flow field is solved with no need of interpolation, while in passive cells no equation is solved because they are temporarily or permanently removed from the calculation. The overset process starts from the hole recognition, which results in the identification of the set of passive cells. The set of Partial Differential Equations (PDEs) characterizing the flow field must be solved on all grids at the same time. For this reason, the results in the background region must be coupled with the ones obtained in the overset grids, interpolating the flow variables between acceptor and donor cells. Acceptor cells mark the boundary of one grid overlapping with another one. The acceptor cells act as ghost cells in the finite volume discretization, so their center only enters into discretized equations of the neighbors. This could cause a gap between the number of equations and the number of variables. This gap is filled by a number of interpolating equations for the values of flow variables at the acceptor cell centers. The donor cells are a set of cells which is employed in the creation of interpolating equations, which can be based on different interpolation methods.

Commercial CFD software houses have been developing the overset mesh technique for several years, but its implementation in OpenFOAM is very recent. This is a new feature in the open-source CFD environment, so its performance and robustness keep increasing with the continuous development.

In the OpenFOAM implementation, the overlapping zone must contain at least 4 cell layers in both background and overset meshes. In applications concerning PDM this constraint originates a relevant issue regarding the mesh size, because of the very small dimensions of gap regions. In order to correctly model the flow inside these machines, several millions of cells should be employed for the discretization of every gap region. On the other hand, the overset technique allows to maintain the grid morphology during the simulation, and the quality of the elements in the gaps remains excellent. Unfortunately, the computational effort associated with the interpolation process and with the high number of cells is unacceptable for numerical simulations of realistic PDM. The unsuitability of this meshing strategy for the applications discussed in this work has been proven by the authors. Figure 1 shows the mesh of a Single-Screw machine characterized by more than 5 millions of elements. Such a number of cells requires a very high computational time for the oversets interpolation process at every time step, but the mesh is far from being refined enough. The figure clearly demonstrates that the size of gap elements is still too big, originating severe errors in the holes recognition process.

The next steps in the development of the overset strategy for PDM could regard the dynamic refinement or the zero-gap approach. In the first case, the mesh could be dynamically refined where the distance between the bodies becomes smaller than a predefined value. On the contrary, the zero-gap approach is involved when the distance between the overset mesh and the background mesh is less than three cells. In this case, such cells are removed from the calculation, the gap is sealed and the minimum requirement of four overlapping cells is not valid anymore.

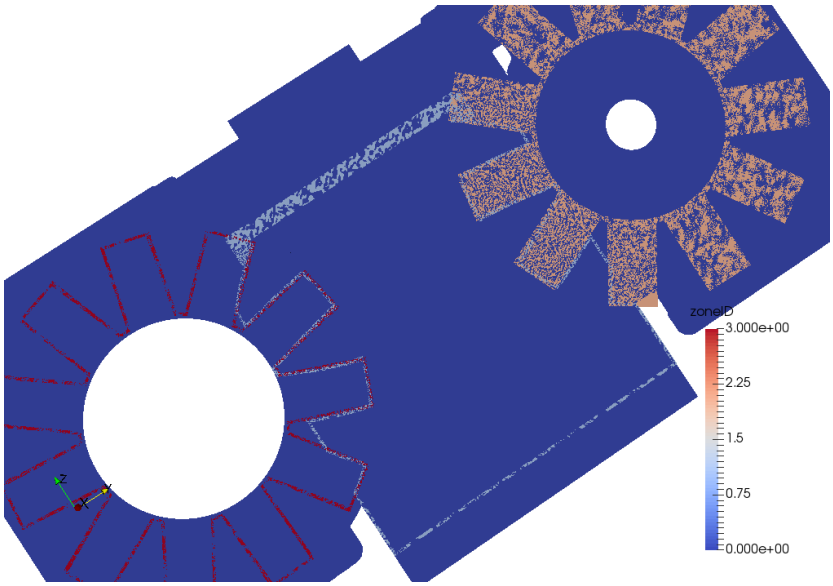

Figure 1. Overset mesh of a SSE: issues in hole recognition.

2.2.3. Mesh Deformation—Mesh Adaption Dynamic Remeshing

The Mesh Adaption Dynamic Remeshing (MADR) is a numerical strategy that includes mesh deformation as a consequence the motion of inner parts. This technique, firstly introduced with the foam-extend version, has been made available to the other branches. However, the compatibility is not guaranteed after OpenFOAM-2.3.x. The algorithm is based on the standard dynamic mesh classes and extends their capability.

In this case, the entire process is divided into three steps: mesh smoothing, mesh reconnecting and mesh remapping [33]. The mesh smoothing step is characterized by no changes in connectivity. This step is introduced to delay the local re-mesh requirement by keeping the mesh quality as high as possible. Indeed, the distortion induced by the displacement of the boundary is smoothed inside the domain. The way this smoothing happens is user-defined by, for example, solving a Laplace/Poisson equation with a user-specified diffusivity. Another option is to get advantage of the Mesquite optimization toolkit [34], which is provided with the MADR library as well. Such mesh morphing techniques force the cells that have a higher quality to deform more than the lower quality cells. The desire is to postpone as much as possible the remeshing phase that is time-consuming and might lead to interpolation errors.

The second step is the mesh reconnecting. This phase occurs when the distortion of the mesh is too big to be handled by the smoothing. The remeshing is local, in the sense that only the cells that have a bad quality are modified. This helps in limiting the interpolation errors that might arise and reduces the computational effort. Besides remeshing, refinement can be introduced. This can be based on mesh quality, length scales or field value. For example, Figure 2 reports a refinement based on length scale. Specifically, it can be noticed that inside the groove a refinement has been imposed. This does not happen outside the groove, in the bulk of the casing, where there is no need of such accurate resolution.

The last step of the algorithm is the mapping of the solution in the old cells into the new generated ones. This is done by storing both the old and new mesh in a single "super" mesh. Then the mapping is done by computing the intersection between the source and the target mesh. At this point, the computation and limitation of the gradients on the source mesh happen. The final step is the volume and distance weighted Taylor series interpolate to super mesh, and finally there is the agglomeration on the target.

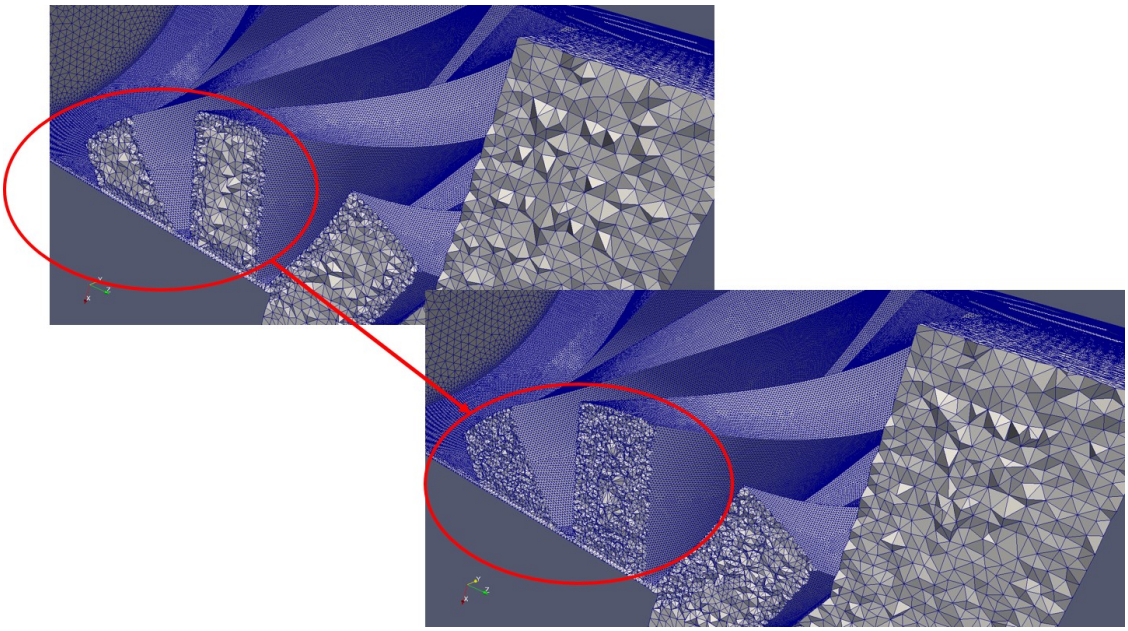

Figure 2. Localized refinement according to length scale.

This approach can bear virtually any kind of deformation, can work very fast and, since the remeshing is only local, the mass conservation error is very small. Nonetheless, it has a few limitations. First, only simplicial cells are supported. Therefore a tetrahedral mesh generator should be employed, and it is not possible to guarantee the alignment at the walls. The other limitations are related to parallel computation, which is not very robust, and the interruption of the libraries' maintenance by the developers.

2.2.4. Mesh Deformation—Key Frame Remeshing

This strategy is similar to the MADR: remeshing is required in order to accommodate excessive cell distortion. This technique, however, is not local as the former one. The complete remeshing of the geometry is required at fixed time intervals. The length of such intervals might be chosen in order to let the smoothing of the mesh (that can be included in this approach) to act for a number of time steps. This would delay the remeshing requirement and would, therefore, help in containing the computational cost of the simulation.

This library is not closely related to any of the branches described above, but it is rather a user-defined algorithm that calls the solver and the mesh generation (or substitute the mesh if already available). Therefore it can be applied to all the different versions of the software. The algorithm requires a set of meshes for the solution of the problem: one mesh is generated, the flow field is solved for a prescribed number of time steps, then the solution is mapped on a new mesh that is generated with the rotating walls that are in the position related to the final time step analyzed by the previous solution. And this procedure is iterated over and over in order to achieve convergence. The number of mesh required for a full simulation of the SS is related to the periodicity of the satellite wheels (and, generally speaking, the rotating part with the lower periodicity interval). The mapping from one mesh to the next occurs calling the *mapFields* utility of OpenFOAM.

This technique is robust and can handle very big mesh distortion. It also has some advantages related to the mesh type that can be handled (arbitrary element shape) and the preserved alignment wall-faces in the boundary layer area. The cons related to this technique are related to the computational effort, that can be very high, and the non-trivial usage (a little coding is necessary for setting up the case). Finally, the conservation of the mass might be not ensured, as the space conservation law is not strictly respected [27].

The Key Frame technique have been applied to the simulation of the SSE. The mesh used for the simulation is an unstructured Cartesian trimmed mesh, composed by roughly 14 millions elements and allows to achieve an average $y+$ of 20.

The surface mesh on the screw has a peculiarity: the wall of the screw has an hole, where contact happens and thus the mesh of the screw is merged with the star wheel mesh. The mesh merging when contact happens is allowed by using the Key Frame remeshing technique by proper choice of the minimum element size. The *snappyHexMesh* utility will therefore merge two surfaces which are closer than that size and thus the contact between the engaging parts can be kept into account. The correct contact detection is important from the stress point of view, but the flow field inside the machine is only slightly affected by this phenomenon.

The results obtained by the usage of such a technique after the passage of one groove are reported in Figure 3. The expansion of the R134a is well represented by the temperature distribution on the flow field. The attention of the reader is driven on the low temperature area downstream the gap. Here the fast expansion of the flow through the gap causes a temperature drop caught by the numerical simulation.

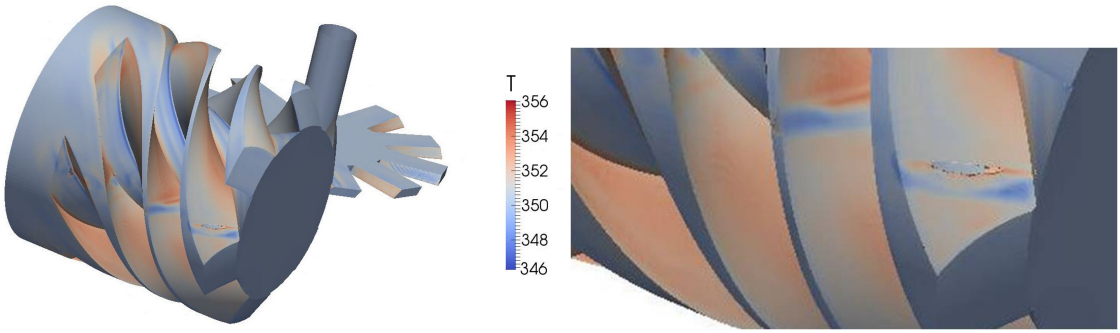

(**a**) (**b**)

Figure 3. Key Frame of Reference results: Temperature pattern on the screw and particular of the engagement area. From [35]. (**a**) Temperature pattern on the screw; (**b**) Temperature pattern downstream the engagement.

As mentioned above, the simulations carried out by employing this technique are affected by error in mass conservation due to space conservation law violation. This error propagates as the number of re-meshing operation increases. It is thus important to reduce as much as possible these occurrences. In this work, for a SSE rotating at 3000 rpm, the maximum interval of time allowed by the set-up employed by the authors is equal to 10 µs. This value derives from a trial and error procedure. this leads to the employment of roughly 300 meshes per pitch. More details are reported in [35].

3. Custom Predefined Mesh Generation—Twin Screw Machines

3.1. Creating and Moving The Mesh

Twin-screw machines are characterized by a simpler geometry than that of single-screw ones. Therefore, it is possible to adopt an alternative approach for the mesh generation, which consists in the realization of body-fitted structured grids. These meshes can be stretched maintaining a good quality of the elements. If the body motion is pre-defined, it is possible to generate a set of structured meshes in advance of the actual simulation. In order to avoid degenerated cells, the nodes of the grid are forced to pass through the control points represented by the nodal coordinates of the pre-defined meshes. One of the major advantages of this strategy is the absence of any form of remeshing or interpolation. For this reason, the space conservation law and mass imbalances due to interpolation processes are not a concern during the simulation. Furthermore, the solution of the flow fields in the nearby of the boundaries is usually satisfying, because the grid is always aligned to the walls.

The realization of structured grids for PDM is not a trivial operation, because of the complex geometry to discretize. There are different meshing software available on the market that proposes different strategies for the generation of structured meshes of PDM. The authors have adopted SCORG-v5.7 for the generation of the grids and OpenFOAM-v1806+ for the computation of the fluid dynamics. SCORG generates the grids for a wide range of PDM, including Twin-Screw and Lobed compressors, see SCORGManual [36] for detailed information. The mesh is created starting from the rotor profiles and gap sizes, then a list of files with the nodal coordinates evolution is provided as output.

The authors have refined the OpenFOAM library SCORGfvMotion, presented in [12], for handling the dynamic mesh motion according to the SCORG output. The machines considered in this work are characterized by a rotating motion, therefore the number of grids set by the user leads to a predefined angular step separating each provided file. Consequently, it is necessary to perform the simulation with a fixed time step, imposed by this angular increment. This constraint may lead to very high Courant-Friedrichs-Lewy (CFL) numbers during the numerical analysis. Hence, the authors have decided to include in the utility the possibility of linearly interpolate between the SCORG grid files, generating intermediate positions. In this way, a variable time step can be adopted and the CFL number is restricted to more reasonable values.

3.2. *Applications: Twin-Screw and Roots Blower*

Casari et al. [12] have applied the method proposed on a Twin-Screw expander with a mild wrap angle. They have encountered several issues related to faces having a wrong oriented normal. These faces were the source of temperature spikes originated on the surfaces of the rotors. In this work, the hexahedral cells generated by SCORG have been split in prisms, as shown in Figure 4. This topological change of the mesh has solved the problem of incorrectly oriented faces. The new approach has been applied to a twin screw compressor with a rotational speed of 8000 rpm, inlet pressure of 1 bar and outlet pressure of 3 bar. The mesh of the machine has been realized with a non-conformal distribution of the points at the interface between the two rotors. For this reason, it has been necessary to set up an Arbitrary Mesh Interface (AMI) [37] in order to interpolate the flow fields.

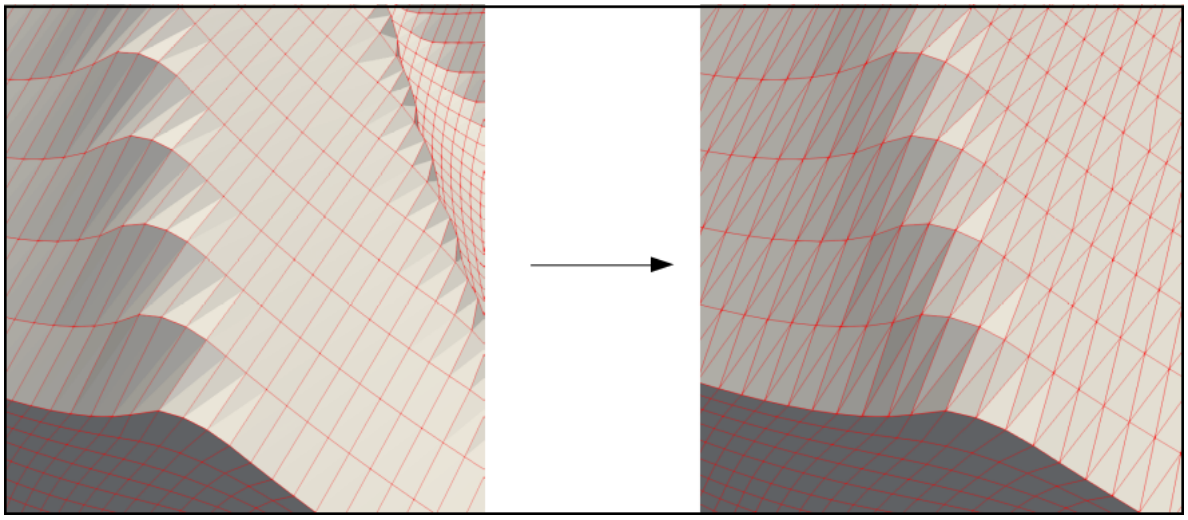

Figure 4. Splitting of hexaedral cells in prisms.

The simulation with prismatic cells has resulted in a drastic reduction of temperature spikes, and in a good pressure distribution represented in Figure 5. Unfortunately, the authors have encountered issues related to mass imbalance, probably due to the behavior of the AMI interface between the two rotors.

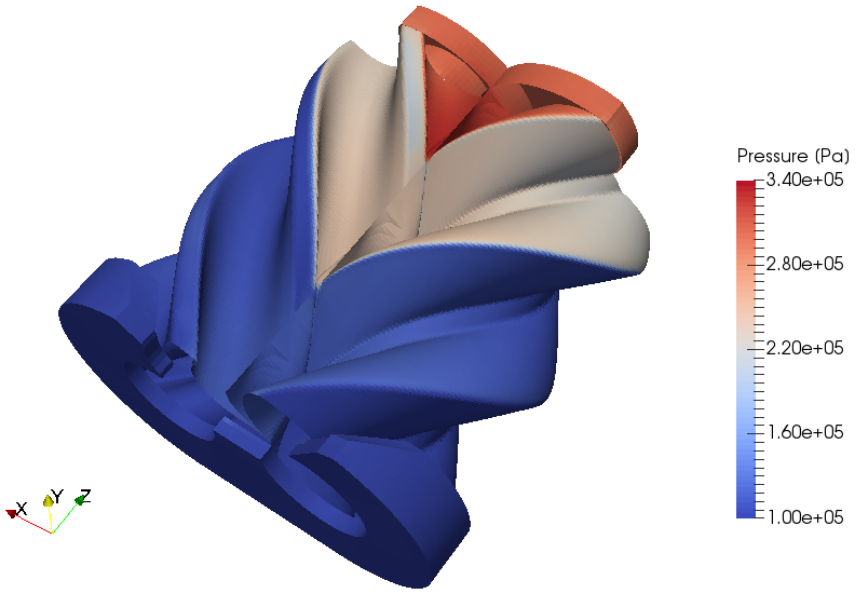

Figure 5. Twin screw pressure distribution.

The last test case presented in this work is the numerical analysis of a Roots Blower compressor. The choice of such machine derives from the intent of simplifying the problem, analyzing a compressor with no wrap angle and higher mesh quality, but maintaining the same mesh motion technique. The nodes distribution at the interface has been realized with a conformal algorithm, in order to remove the interface effects. The mesh used for the investigation is reported in Figure 6. The refinement close to the wall might be achieved by forcing the mesh to have a different grading when approaching the wall.

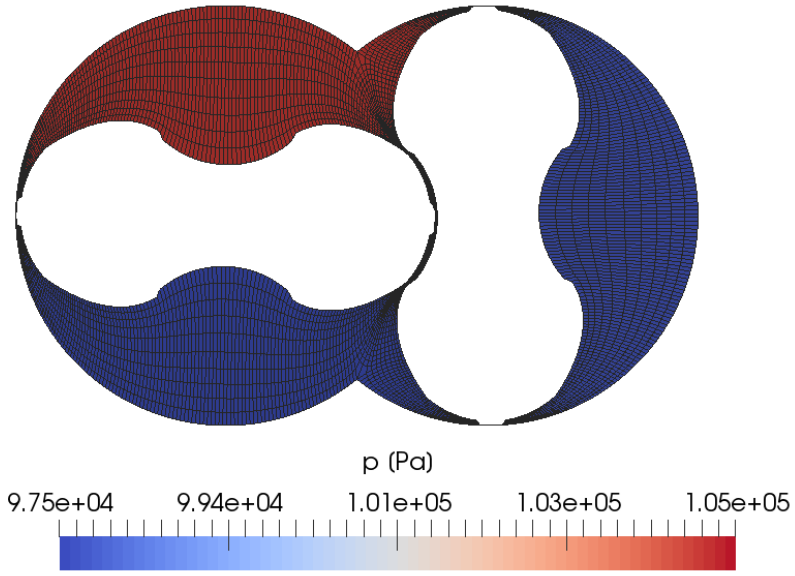

Figure 6. Roots blower: structured grid and pressure contour.

This is not crucial in this kind of machine as the squeezing of the mesh in the gaps reduces the first layer thickness and helps in keeping the y^+ in the ideal region. The analysis has produced

satisfying results, whit a discrete accordance of the mass flow rate, shown in Figure 7, with the one measured in [38]. The values derived from the numerical simulation are definitely higher, but it must be considered that no axial gaps have been modeled in the current analysis.

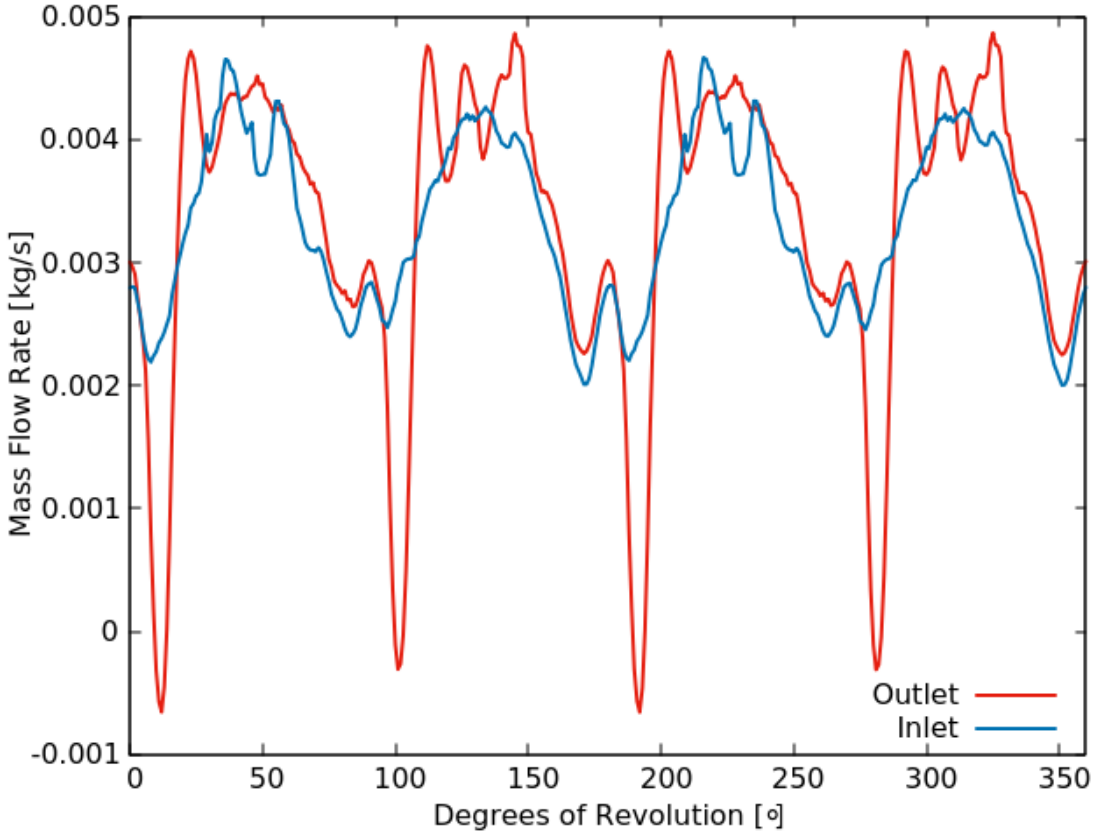

Figure 7. Roots blower: mass flow rate.

3.3. OpenFOAM Thermophysical Models

The computation of thermophysical properties in an OpenFOAM simulation is based on a pressure-temperature system. These variables are the independent variables, from which other properties are determined. Frequently, the user has to evaluate thermophysical properties in applications where the ideal gas approximation is not usable with reasonable accuracy. In such cases, the most accurate model for the evaluation of the fluid density is the Peng-Robinson (PR) equation of state, one of the most common cubic models:

$$p = \frac{RT}{\nu - b} - \frac{a_c \alpha(T_R, \omega)}{\nu(\nu + b) + b(\nu - b)} \tag{1}$$

with the parameters:

$$a_c = 0.45724 \left(\frac{R^2 T_C^2}{P_C} \right)$$

$$b = 0.07780 \left(\frac{RT_C}{P_C} \right)$$

$$\alpha(T_R, \omega) = \left[1 + m(\omega) \left(1 - \sqrt{T_R} \right) \right]^2$$

$$m(\omega) = 0.37464 + 1.54226\omega - 0.26992\omega^2$$

where v is the molar volume, T_R is the reduced temperature, ω is the acentric factor, R is the gas constant, and T_C and P_C are the critical values of temperature and pressure, respectively. PR is quite accurate in different conditions, but for saturated liquid densities, conditions close to critical point and caloric properties in the homogeneous region the error increases [39,40]. Nevertheless, PR and other cubic equations of state are frequently adopted for the evaluation of vapor pressures and equilibrium-phase compositions of mixtures. In such cases, these equations of state need less computational resources than multiparameter equations of state [41], yielding relatively accurate results. In CFD analysis, the computational overhead has to be taken into account, evaluating different fluid property models on a case-by-case basis. Cubic EOS may represent an effective trade-off between accuracy and computational load, as pointed out by Abdelli et al. [42].

It is also possible to adopt a polynomial model, where the density trend is fitted with constant pressure and the temperature as the independent variable. Polynomial functions inherently lack accuracy in the presence of wide pressure ranges and phase change, as well as density trends difficult to shape. Polynomials are usable also for the specific heat and transport properties (viscosity, thermal conductivity and thermal diffusivity). Thermodynamic properties, which are derived from the specific heat, can be also evaluated from the JANAF tables of thermodynamics [43]. In addition to that, the Sutherland model for the transport properties calculation is available. Again, wide pressure ranges and complex trends of the variables can be significant sources of inaccuracy.

3.4. CoolProp Thermophysical Models

CoolProp is the most spread open source library for the determination of thermophysical properties. The thermodynamic characterization of the fluids included in the library is built on equations of state explicit in the Helmholtz energy [22]. The nondimensionalized Helmholtz-energy can be decomposed in a residual part (α^r) and an ideal gas part (α^0):

$$\alpha = \alpha^0 + \alpha^r \tag{2}$$

One important feature of this formulation is that all the other thermodynamic properties can be calculated through the derivatives of the two Helmholtz-energy terms. For instance, the pressure can be estimated as follows:

$$Z = \frac{p}{\rho RT} = 1 + \delta \left(\frac{\partial \alpha^r}{\partial \delta} \right)_\tau \tag{3}$$

where R is the mass specific gas constant, p is the pressure, Z is the compressibility factor, T is the temperature, ρ is the density, δ is the reciprocal reduced temperature given by $\tau = T_{red}/T$ and the reduced density is $\delta = \rho/\rho_{red}$. Usually the reducing variables ρ_{red} and T_{red} refer to the critical point values. More information about the derivatives of the Helmholtz formulation can be found in literature works of authors such as Thorade and Sadat [44], Span [45] and Lemmon [46].

For the evaluation of transport properties the state there is a wide range of methods available in the literature. Highly accurate formulations are available for some fluids, but in other cases the offer is definitely scarce. The divergence of viscosity values close to the critical point is known as critical enhancement [47]. In CoolProp this phenomenon is considered only for water [48] and carbon dioxide [49], because for the majority of fluids it is negligible. Oppositely, for the thermal conductivity the critical enhancement has been observed for temperatures up to 20% higher than the critical one. Consequently, the thermal conductivity formulations contain a special term in order to take this deviation into account.

Fadiga et al. [50] have developed a wrapper of the CoolProp library for OpenFOAM. This wrapper represents a good option when the maximum accuracy is required, but the computational effort is definitely higher. The implementation is particularly easy to use, since it requires only the fluid name to be provided. The experimental case used for the validation is the convergent-divergent nozzle of the TROVA test rig on the expansion of octamethyltrisiloxane (MDM) in a convergent-divergent

nozzle, reported in Spinelli et al. [51]. The work investigates two nozzles, characterized by downstream Mach numbers close to 1.5 and 2. The first nozzle's results are considered in this section: particularly, the case with upstream compressibility Z of approximately 0.81 is the object of the numerical analysis. The considered gas is then strongly non-ideal: this allows the full demonstration of the CoolFOAM interface potentialities.

Since the fluid reaches supersonic velocities, there is no need of boundary conditions at the outlet section. At the inlet, a total pressure of 4.59 bar and a total temperature of 512.6 K have been imposed. The solution has been firstly initialized with ideal gas conditions, switching then to the Helmholtz equation of state. After this first step, the hypothesis of inviscid flow has been considered valid for this kind of fluid, characterized by a very low viscosity. The simulation with zero viscosity and laminar approximation has produced very good results when compared to the experimental data, as shown in Figure 8.

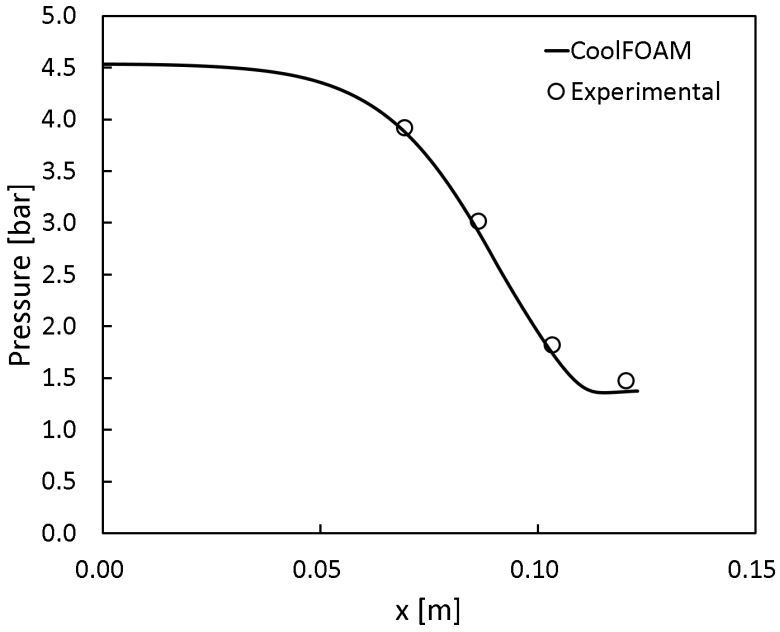

Figure 8. Convergent-divergent nozzle: pressure values on the symmetry axis, inviscid flow.

4. Conclusions

The authors have described, tested and analyzed the applicability of OpenFOAM with the dynamic simulations of PDMs. A thorough review of the state of the art techniques available with the software for the simulation of such devices is reported here. The possibilities the software suite offers for the simulation are several: immersed boundaries, overset, dynamic remeshing and key frame remeshing. Unfortunately, the rough and ready applicability of the technique presented here is not guaranteed. Each of the approaches has some flaws that make its usage not straightforward.

A the moment, concerning the SSE, two techniques seem the most promising, and these will receive attention by the authors as a follow-up of this analysis: the immersed boundary method and the mesh adaption—dynamic remeshing. The overset approach will require some extra testing and refining by the developers. The key frame remeshing is extremely time-consuming and therefore its applicability is limited.

The custom predefined mesh generation strategy is the most indicated choice for the simulation of PDM, when the geometry is simple enough to be discretized with a structured mesh. This provides many advantages such as accuracy and mass conservation, that are typically difficult to achieve with other methods. The authors have shown the applicability of this method for a twin screw and a roots blower. Furthermore, the authors have reviewed the thermophysical modeling capabilities of

OpenFOAM, with particular care to real gas properties. In addition to that, a new interface between CoolProp and OpenFOAM has been added to the software possibilities.

Author Contributions: A.S., E.F. and N.C. methodology & conceptualization, N.C. writing original draft; E.F. and N.C. software and data curation; M.P. and D.Z. supervision and funding acquisition; D.Z. writing–review & editing. All authors have read and agreed to the published version of the manuscript.

Funding: The research was partially supported by *PDM Analysis* and the Italian Ministry of Economic Development within the framework of the Program Agreement MSE-CNR "Micro co/tri generazione di Bioenergia Efficiente e Stabile (Mi-Best)".

Acknowledgments: The authors would like to thank *PDM Analysis* for the financial support and the possibility of publishing this work.

Conflicts of Interest: The authors declare no conflict of interest.

References

1. Macchi, E.; Astolfi, M. *Organic Rankine Cycle (ORC) Power Systems, Technologies and Applications*; Woodhead Publishing Series in Energy; Woodhead Publishing: Duxford, UK, 2016; Volume 107.
2. Montenegro, G.; Della Torre, A.; Onorati, A.; Broggi, D.; Schlager, G.; Benatzky, C. *CFD Simulation of a Sliding Vane Expander Operating inside a Small Scale ORC for Low Temperature Waste Heat Recovery*; Technical Report, SAE Technical Paper; SAE International: Warrendale, PA, USA, 2014.
3. Kovacevic, A.; Stosic, N.; Smith, I. *Screw Compressors: Three Dimensional Computational Fluid Dynamics and Solid Fluid Interaction*; Springer Science & Business Media: Berlin/Heidelberg, Germany, 2007; Volume 46.
4. Mujic, E.; Kovacevic, A.; Stosic, N.; Smith, I. The influence of port shape on gas pulsations in a screw compressor discharge chamber. *Proc. Inst. Mech. Eng. Part E J. Process Mech. Eng.* **2008**, *222*, 211–223. [CrossRef]
5. Tang, H.; Wu, H.; Wang, X.; Xing, Z. Performance study of a twin-screw expander used in a geothermal organic Rankine cycle power generator. *Energy* **2015**, *90*, 631–642. [CrossRef]
6. Ziviani, D.; Groll, E.A.; Braun, J.E.; De Paepe, M. Review and update on the geometry modeling of single-screw machines with emphasis on expanders. *Int. J. Refrig.* **2018**, *92*, 10–26. [CrossRef]
7. Stosic, N.; Smith, I.K.; Kovacevic, A. A twin screw combined compressor and expander for CO_2 refrigeration systems. In Proceedings of the International Compressor Engineering Conference, West Lafayette, Indiana, 16–19 July 2002.
8. Lemort, V.; Guillaume, L.; Legros, A.; Declaye, S.; Quoilin, S. A comparison of piston, screw and scroll expanders for small scale Rankine cycle systems. In Proceedings of the 3rd International Conference on Microgeneration and Related Technologies, Napoli, Italy, 15–17 April 2013.
9. Montenegro, G.; Della Torre, A.; Onorati, A.; Broggi, D.; Schlager, G.; Benatzky, C. *Directive 2005/32/EC Establishing a Framework for the Setting of Ecodesign Requirements for Energy-Using Products and Amending Council Directive 92/42/EEC and Directives 96/57/EC and 2000/55/EC. OJ, 2005; L191/29*; Technical Report; European Parliament: Brussels, Belgium, 2009.
10. Kennedy, S.; Wilson, M.; Rane, S. *Combined Numerical and Analytical Analysis of an Oil-Free Twin Screw Compressor*; IOP Conference Series: Materials Science and Engineering; IOP Publishing: Bristol, UK, 2017; Volume 232, p. 012080.
11. Sun, S.; Kovacevic, A.; Bruecker, C.; Leto, A.; Singh, G.; Ghavami, M. *Numerical and Experimental Analysis of Transient Flow in Roots Blower*; IOP Conference Series: Materials Science and Engineering; IOP Publishing: Bristol, UK, 2018; Volume 425, p. 012024.
12. Casari, N.; Pinelli, M.; Suman, A.; Kovacevic, A.; Rane, S.; Ziviani, D. *Full 3D Numerical Analysis of a Twin Screw Compressor by Employing Open-Source Software*; IOP Conference Series: Materials Science and Engineering; IOP Publishing: Bristol, UK, 2018; Volume 425, p. 012017.
13. Randi, S.; Suman, A.; Casari, N.; Pinelli, M.; Ziviani, D. *Numerical Analysis of Oil Injection Effects in a Single Screw Expander*; IOP Conference Series: Materials Science and Engineering; IOP Publishing: Bristol, UK, 2018; Volume 425, p. 012001.
14. Suman, A.; Ziviani, D.; Gabrielloni, J.; Pinelli, M.; De Paepe, M.; Van Den Broek, M. Different Numerical Approaches for the Analysis of a Single Screw Expander. *Energy Procedia* **2016**, *101*, 750–757. [CrossRef]

15. Morini, M.; Pavan, C.; Pinelli, M.; Romito, E.; Suman, A. Analysis of a scroll machine for micro ORC applications by means of a RE/CFD methodology. *Appl. Therm. Eng.* **2015**, *80*, 132–140. [CrossRef]
16. Chang, J.C.; Chang, C.W.; Hung, T.C.; Lin, J.R.; Huang, K.C. Experimental study and CFD approach for scroll type expander used in low-temperature organic Rankine cycle. *Appl. Therm. Eng.* **2014**, *73*, 1444–1452. [CrossRef]
17. Lemmon, E.W.; Tillner-Roth, R. A Helmholtz energy equation of state for calculating the thermodynamic properties of fluid mixtures. *Fluid Phase Equilibria* **1999**, *165*, 1–21. [CrossRef]
18. Peng, D.Y.; Robinson, D.B. A new two-constant equation of state. *Ind. Eng. Chem. Fundam* **1976**, *15*, 59–64. [CrossRef]
19. Redlich, O.; Kwong, J.N. On the thermodynamics of solutions. V. An equation of state. Fugacities of gaseous solutions. *Chem. Rev.* **1949**, *44*, 233–244. [CrossRef]
20. Aungier, R. A fast, accurate real gas equation of state for fluid dynamic analysis applications. *Trans.-Am. Soc. Mech. Eng. J. Fluids Eng.* **1995**, *117*, 277. [CrossRef]
21. Soave, G. Equilibrium constants from a modified Redlich-Kwong equation of state. *Chem. Eng. Sci.* **1972**, *27*, 1197–1203. [CrossRef]
22. Bell, I.H.; Wronski, J.; Quoilin, S.; Lemort, V. Pure and pseudo-pure fluid thermophysical property evaluation and the open-source thermophysical property library CoolProp. *Ind. Eng. Chem. Res.* **2014**, *53*, 2498–2508. [CrossRef] [PubMed]
23. snappyHexMesh Algorithm. Available online: https://cfd.direct/openfoam/user-guide/v6-snappyhexmesh/ (accessed on 1 October 2019).
24. Juretić, F. *cfMesh User Guide*; Creative Fields: Zagreb, Croatia, 2015.
25. Bergeaud, V.; Lefebvre, V. SALOME. A software integration platform for multi-physics, pre-processing and visualisation. In Proceedings of the Joint International Conference on Supercomputing in Nuclear Applications and Monte Carlo, Tokyo, Japan, 17–21 October 2010.
26. Geuzaine, C.; Remacle, J.F. *Gmsh Reference Manual*; Free Software Foundation Inc.: Boston, MA, USA, 2003.
27. Ferziger, J.H.; Perić, M. *Computational Methods for Fluid Dynamics*; Springer: Berlin/Heidelberg, Germany, 2002; Volume 3.
28. Peskin, C.S. Flow Patterns around Heart Valves: A Digital Computer Method for Solving the Equations of Motion. Ph.D. Thesis, Yeshiva University, New York, NY, USA, 1972.
29. Mittal, R.; Iaccarino, G. Immersed boundary methods. *Annu. Rev. Fluid Mech.* **2005**, *37*, 239–261. [CrossRef]
30. Jasak, H.; Tukovic, Z. Immersed Boundary Method in FOAM: Theory, Implementation and Use. Available online: http://www.tfd.chalmers.se/~hani/kurser/OS_CFD_2015/H-rvojeJasak/ImmersedBoundary.pdf (accessed on 1 January 2015).
31. Benek, J.; Steger, J.; Dougherty, F.C. A flexible grid embedding technique with application to the Euler equations. In Proceedings of the 6th Computational Fluid Dynamics Conference Danvers, Danvers, MA, USA, 13–15 July 1983; p. 1944.
32. Benek, J.; Buning, P.; Steger, J. A 3-D chimera grid embedding technique. In Proceedings of the 7th Computational Physics Conference, Cincinnati, OH, USA, 15–17 July 1985; p. 1523.
33. Menon, S.; Mooney, K. Using the dynamicTopoFvMesh class in OpenFOAM. Available online: www.personal.psu.edu/dab143/OFW6/Training/mooney_slides.pdf (accessed on 30 January 2020).
34. Brewer, M.L.; Diachin, L.F.; Knupp, P.M.; Leurent, T.; Melander, D.J. The Mesquite Mesh Quality Improvement Toolkit. In Proceedings of the 12th International Meshing Roundtable, IMR, Santa Fe, NM, USA, 14–17 September 2003.
35. Casari, N.; Suman, A.; Ziviani, D.; Van Den Broek, M.; De Paepe, M.; Pinelli, M. Computational Models for the Analysis of positive displacement machines: Real Gas and Dynamic Mesh. *Energy Procedia* **2017**, *129*, 411–418. [CrossRef]
36. *SCORG V5.7 Manual*; PDM Analysis Ltd.: Barnet, UK, 2019. Available online: http://pdmanalysis.co.uk/online-documentation/online-documentation/ (accessed on 7 September 2019).
37. Farrell, P.; Maddison, J. Conservative interpolation between volume meshes by local Galerkin projection. *Comput. Methods Appl. Mech. Eng.* **2011**, *200*, 89–100. [CrossRef]
38. Singh, G.; Sun, S.; Kovacevic, A.; Li, Q.; Bruecker, C. Transient flow analysis in a Roots blower: Experimental and numerical investigations. *Mech. Syst. Signal Process.* **2019**, *134*, 106305. [CrossRef]

39. Kunz, O.; Wagner, W. The GERG-2008 Wide-Range Equation of State for Natural Gases and Other Mixtures: An Expansion of GERG-2004. *J. Chem. Eng. Data* **2012**, *57*, 3032–3091. [CrossRef]
40. Valderrama, J. The state of the cubic equations of state. *Ind. Eng. Chem. Res.* **2003**, *42*, 1603–1618. [CrossRef]
41. Gernert, J.; Jäger, A.; Span, R. Calculation of phase equilibria for multi-component mixtures using highly accurate Helmholtz energy equations of state. *Fluid Phase Equilibria* **2014**, *375*, 209–218. [CrossRef]
42. Lazhar Abdelli, J.D.; Vierendeels, J. CFD Analysis of an Expansion Process Using Different Real Gas Models. Master's Thesis, Ghent University, Ghent, Belgium, 2015.
43. Allison, T. *JANAF Thermochemical Tables, NIST Standard Reference Database 13*; NIST: Gaithersburg, MD, USA, 1996. [CrossRef]
44. Thorade, M.; Saadat, A. Partial derivatives of thermodynamic state properties for dynamic simulation. *Environ. Earth Sci.* **2013**, *70*, 3497–3503. [CrossRef]
45. Span, R. *Multiparameter Equations of State*; Springer: Berlin/Heidelberg, Germany, 2000. [CrossRef]
46. Lemmon, E.; Jacobsen, R.; Penoncello, S.; Friend, D. Thermodynamic properties of air and mixtures of nitrogen, argon, and oxygen from 60 to 2000 K at pressures to 2000 MPa. *J. Phys. Chem. Ref. Data* **2000**, *29*, 331–362. [CrossRef]
47. Sengers, J. Transport properties of fluids near critical points. *Int. J. Thermophys.* **1985**, *6*, 203–232. [CrossRef]
48. Huber, M.L.; Perkins, R.A.; Laesecke, A.; Friend, D.G.; Sengers, J.V.; Assael, M.J.; Metaxa, I.N.; Vogel, E.; Mareš, R.; Miyagawa, K. New International Formulation for the Viscosity of H2O. *J. Phys. Chem. Ref. Data* **2009**, *38*, 101–125. [CrossRef]
49. Bock, S.; Bich, E.; Vogel, E.; Dickinson, A.S.; Vesovic, V. Calculation of the transport properties of carbon dioxide. III. Volume viscosity, depolarized Rayleigh scattering, and nuclear spin relaxation. *J. Chem. Phys.* **2004**, *121*, 4117–4122. [CrossRef] [PubMed]
50. Fadiga, E.; Casari, N.; Suman, A.; Pinelli, M. CoolFOAM: The CoolProp wrapper for OpenFOAM. *Comput. Phys. Commun.* **2019**. [CrossRef]
51. Spinelli, A.; Cammi, G.; Gallarini, S.; Zocca, M.; Cozzi, F.; Gaetani, P.; Dossena, V.; Guardone, A. Experimental evidence of non-ideal compressible effects in expanding flow of a high molecular complexity vapor. *Exp. Fluids* **2018**, *59*. [CrossRef]